Materials Science in Semiconductor Processing 185 (2025) 109011

Contents lists available at ScienceDirect

Materials Science in Semiconductor Processing

journal homepage: www.elsevier.com/locate/mssp

On the absorption coefficient of $GaP_{1-x}N_x$ layers and its potential application for silicon photovoltaics

K. Ben Saddik [a,1], M.J. Hernández [a,b,c,d,*], M.A. Pampillón [a,b,c,d], M. Cervera [a,b,c,d], B.J. García [a,b,c,d]

[a] Semiconductors and Electronics Group (ElySe), Applied Physics Department, Universidad Autónoma de Madrid, C/ Francisco Tomás y Valiente 7, 28049, Madrid, Spain
[b] Instituto Nicolas Cabrera, Universidad Autónoma de Madrid, ES-28049, Madrid, Spain
[c] Centro de Microanálisis de Materiales (CMAM), Universidad Autónoma de Madrid, ES-28049, Madrid, Spain
[d] Centro de Investigación Avanzada en Física Fundamental (CIAFF), Universidad Autónoma de Madrid, ES-28049, Madrid, Spain

ARTICLE INFO

Keywords:
III-V alloys
Dilute nitrides
Solar cells
Spectroscopic ellipsometry
Absorption coefficient
Band anticrossing

ABSTRACT

The absorption coefficient and the energy gap of $GaP_{1-x}N_x$ layers has been obtained by spectroscopic ellipsometry for samples grown on Si(001) substrates by chemical beam epitaxy with N mole fractions in the range $0 \leq x \leq 0.081$. The resulting absorption spectra exhibit a direct band-like behavior near the absorption edge. The absorption coefficient values increase with the N content, reaching values in the range $\alpha \sim 1\text{-}2x10^4$ cm^{-1} in the vicinity of the absorption edge below the original GaP direct bandgap, which are comparable to those obtained for high efficiency solar cell materials. Furthermore, dependence of the absorption coefficient with increasing N content points to a strong GaP Γ-like character of the conduction-band wave function of $GaP_{1-x}N_x$ alloys near the Brillouin zone center at $\boldsymbol{k} = 0$, as predicted by the band anticrossing model. Bandgap energy values obtained by spectroscopic ellipsometry are compared with previous values obtained by photoluminescence measurements on the same samples, observing a shift of about 50–100 meV. Finally, the value of the band anticrossing parameter coupling the N level and the host GaP conduction band has been obtained from the dependence of both, the bandgap and the absorption coefficient, with the N content (2.1 and 3.3 eV respectively).

1. Introduction

When host atoms of highly-mismatched alloys are partially replaced by isoelectronic impurities with very different electronegativity and/or ionic radius [1], resulting alloys are characterized by a strong nonlinear dependence of some of their properties on the chemical composition. This is the case of the ternary semiconductor $GaP_{1-x}N_x$, usually obtained as a dilute nitride by the addition of a small N mole fraction, x, into GaP. The incorporation of a small N content not only reduces the alloy lattice parameter, but also reduces its bandgap energy and remarkably induces an indirect-to-direct bandgap transition. While the first effect is linear on x value and can be described by the Vegard law, the changes induced in the bandgap energy are described by the band anticrossing model (BAC) [2].

The material quality of dilute nitrides is known to degrade as the N content and the layer thickness are increased, because of the strain relaxation due to the elastic energy accumulated in the layer. The creation of antiphase domains, induced during the growth of polar on non-polar semiconductors, also limits the integration of $GaP_{1-x}N_x$ based devices with the standard Si technology. We have recently shown that good quality $GaP_{1-x}N_x$ layers with $x \leq 0.04$ can be grown by chemical beam epitaxy (CBE) on CMOS-compatible GaP-on-Si(001) substrates, obtaining chemically homogeneous and flat $GaP_{1-x}N_x$ layers [3,4].

For $x = 0.021$, $GaP_{1-x}N_x$ is lattice matched to Si with a direct bandgap energy of about 1.95 eV at room temperature; larger values of x allow for smaller bandgap energies, while the tensile strain associated to the extra N content may be compensated by the addition of either As or In to form a quaternary alloy, which further reduces the bandgap [5,6]. The above properties make this material system particularly interesting for photovoltaic applications, where it can be integrated in double- and

* Corresponding author. Semiconductors and Electronics Group (ElySe), Applied Physics Department, Universidad Autónoma de Madrid, C/ Francisco Tomás y Valiente 7, 28049, Madrid, Spain.
E-mail address: maria.jesus.hernandez@uam.es (M.J. Hernández).
[1] Present address: LAAS-CNRS, Université de Toulouse, CNRS, 7 Avenue du Colonel Roche, 31400, Toulouse, France.

https://doi.org/10.1016/j.mssp.2024.109011
Received 22 May 2024; Received in revised form 10 October 2024; Accepted 11 October 2024
Available online 16 October 2024

triple-junction solar cells with almost perfect bandgap combinations to maximize the photoconversion efficiency when grown on top of a Si bottom cell (1.1/1.7 eV and 1.1/1.5/2.0 eV, respectively) [7].

An issue of great interest for photovoltaic applications is to know the dependence of the absorption coefficient on the N content of the $GaP_{1-x}N_x$ layer. In our knowledge, there are no experimental studies about the trend of the absorption coefficient and the strength of the optical absorption when changing the N mole fraction. There are only a few published experimental works [8–10] on the optical absorption of $GaP_{1-x}N_x$ and $GaP_{1-x-y}As_yN_x$ alloys for different N contents; although they report results on the shift of the absorption threshold, the behavior of the strength of the optical absorption is still unclear.

In this work, we present some optical properties of $GaP_{1-x}N_x$ layers grown by CBE on nominally (001)-oriented GaP-on-Si substrates using spectroscopic ellipsometry (SE) and photoluminescence (PL). We show the absorption coefficient spectra of $GaP_{1-x}N_x$ behave as expected for a direct bandgap semiconductor. As the bandgap energy value decreases with the N content, the absorption coefficient increases progressively. The absorption coefficient shows a fast increase for energies higher than the absorption edge, reaching typical values in the range 1-2x10^4 cm^{-1} in the vicinity of the absorption edge, located below the original GaP direct bandgap, even for moderate N contents ($x \leq 0.04$), allowing the use of thin epitaxial $GaP_{1-x}N_x$ layers as absorbers on Si-based tandem solar cells. Finally, a simple dependence for the strength of the optical absorption of $GaP_{1-x}N_x$ on N mole fraction is proposed, based on the BAC model.

2. Experimental

$GaP_{1-x}N_x$ layers were grown on GaP-on-Si (001) templates supplied by $NAsP_{III/V}$ GmbH. The thickness of the undoped GaP template layer, free of antiphase boundaries, was 31 nm as measured by X-ray reflectometry (XRR). $GaP_{1-x}N_x$ growth was performed by CBE in a Riber CBE32 system using triethylgallium (TEGa), tertiarybutylphosphine (TBP) and 1,1-dimethylhydrazine (DMHy) as precursors for Ga, P, and N, respectively, by means of a pressure regulated flux control system. TBP was injected through a high temperature cracking cell ($T = 820$ °C) while TEGa and DMHy were supplied through separated low temperature cells ($T = 120$ °C) to avoid pre-cracking of these precursors inside their cells, allowing Ga and N precursors to decompose at the sample surface during growth. Sample temperature was measured using a dual band optical pyrometer and a non-contact thermocouple.

Prior to sample growth, the native oxide layer covering the GaP template was thermally desorbed at the substrate temperature T_s = 610 °C, under TBP flux, until a clear (2 x 4) surface reconstruction was observed by reflection high-energy electron diffraction (RHEED), indicating a null or negligeable density of antiphase domains and boundaries.

An initial GaP buffer layer of 15 nm was grown on each sample at T_s = 580 °C, before the growth of the final $GaP_{1-x}N_x$ epitaxial layer at T_s between 475 and 550 °C during 1 h. Expected thicknesses of the $GaP_{1-x}N_x$ layers were 220 nm, as deduced from the frequency of the RHEED specular spot intensity oscillations during growth, from transmission electron microscopy (TEM) measurements and XRR [3]. TBP and TEGa fluxes were kept fixed for every sample, while the DMHy flux was increased from one sample to the other in the sample set to enhance N incorporation. N contents for the set of samples studied in this work were in the range $0 \leq x \leq 0.081$, according to both, high resolution X-ray diffraction (HRXRD) and nuclear reaction analysis previous results [4]. In case of phase-separated layers, the x value means an average of both N mole fractions.

Samples were analyzed by SE in air with a Woollam rotating compensator ellipsometer (M2000 model) for photon energies between 0.7 and 5.9 eV at an angle of incidence of 75° with a light spot size on the samples of ~3 × 1 mm^2. The own instrument software was used for data fitting and model simulation.

For the lower photon energies between 0.7 and 1.2 eV the Si substrate cannot be considered as a true substrate from the ellipsometric point of view, due to the Si substrate transparency for photon energies below the bandgap energy; the spectra in this region exhibited multiple oscillations caused by light reflection in the backside of the Si substrate. To avoid complicated simulations, SE measurements for samples with $x \neq 0$ have been modeled only in the region of interest for the purpose of this work, between 1.2 and 5.9 eV, using a three-layer model plus a substrate, as shown in Fig. 1.

To reduce the number of unknows during sample modeling by SE, dielectric constants values obtained by Herzinger et al. [11] and Zollner [12] were taken as library spectra for the Si substrate, and for Ga and P oxides (referred as GaP oxide), respectively.

Dielectric functions (DF) $\varepsilon = \varepsilon_1 + i \cdot \varepsilon_2$ of bulk GaP and GaP strained layer on silicon may be slightly different near critical points, due to the effect of strain on semiconductor band structure. Since the use of GaP bulk libraries for the strained buffer layer of our samples could distort the DF obtained for our $GaP_{1-x}N_x$ layers, we have used our own GaP DF library. It has been obtained from the analysis of the spectrum measured for a test GaP sample grown by CBE under the same conditions than GaP buffer layers, but without DMHy flux ($x = 0$) in the same energy range, as explained below. The model shown in Fig. 1 has been reduced to a double-layer model plus a substrate for this sample, because the GaP epilayer and GaP buffer layer merge in a thicker single layer, where the DF of the GaP layer and the thicknesses of both, the GaP and the oxide layers, are the fitting parameters.

A 3rd order basis-spline curve approach was considered to obtain a smooth DF for all $GaP_{1-x}N_x$ layers, using the model of Fig. 1. Kramers-Kronig consistency between the real and imaginary parts of the DF was also imposed to get a physical meaning function, while the imaginary part of the DF was forced to be positive or null. Contributions outside the measured spectra have also been considered by means of two additional fitting parameters accounting for the absorption at the lowest and highest energies on the spectra. An angle offset was also defined as a fitting parameter to compensate for small alignment errors, and the energy range for each spline was fixed at 0.1 eV. The reduction of the spline interval below the above value (50 and 20 meV) produces spurious oscillations in the DF without any noticeable resolution increase. Goodness of fit was quantified by the mean squared error (MSE), defined as:

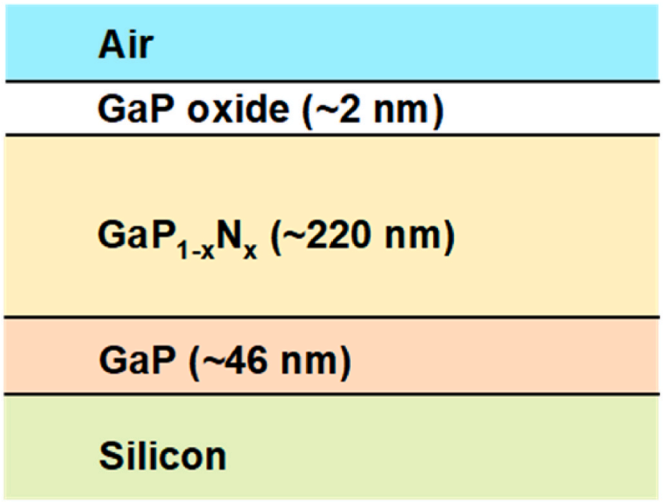

Fig. 1. Three-layer model for SE measurements. Si and GaP oxide DF have been taken from the literature, while GaP DF has been obtained by numerical fitting of the SE measurement of a GaP/Si sample to a reduced two-layer model.

$$MSE = \sqrt{\frac{1}{3n-m}\sum_{i=1}^{n}\left[(N_{Ei}-N_{Gi})^2+(C_{Ei}-C_{Gi})^2+(S_{Ei}-S_{Gi})^2\right]} \times 1000 \quad (1)$$

where n is the number of measurements taken at different wavelengths, m is the number of fit parameters, and $N = \cos(2\Psi)$, $C = \sin(2\Psi)\cdot\cos(\Delta)$, $S = \sin(2\Psi)\cdot\sin(\Delta)$ are functions of the ellipsometric magnitudes Ψ and Δ, in turn dependent on the optical properties of the sample. Subscripts "E" and "G" refer to experimental and generated magnitudes, respectively. MSE values below 10 are indicative of an acceptable fitting and modeling for multilayer samples as those used in this work.

Once obtained the DF of GaP, those of $GaP_{1-x}N_x$ layers have been obtained by fitting the spectra of these samples to the model shown in Fig. 1, with the thickness of the GaP layer as an additional fitting parameter.

3. Results and discussion

According to the described data analysis procedure, MSE obtained values for the best fittings of the DF were between 1.5 and 3.2 for the set of samples. For instance, Fig. 2 shows the experimental and generated Ψ and Δ curves for a sample containing a $GaP_{1-x}N_x$ layer with $x = 0.024$. Thicknesses obtained for GaP, $GaP_{1-x}N_x$ and GaP oxide layers were 45 nm, 219 nm and 2.1 nm, respectively, in good agreement with the expected values. Fits with similar quality, not shown here for simplicity, have been obtained for spectra of the sample set studied in this work.

Using the well-known relations between the DF and the absorption coefficient α

$$\varepsilon_2 = 2nk, \alpha = \frac{4\pi k}{\lambda} \quad (2)$$

absorption coefficient spectra for $GaP_{1-x}N_x$ layers may be obtained. Fig. 3 shows a plot of the absorption coefficient spectra as a function of the photon energy, in the vicinity of the absorption edge, for the most representative $GaP_{1-x}N_x$ layers along with that of GaP ($x = 0$). Samples with N content greater than $x = 0.04$ were identified in a previous work as phase-separated $GaP_{1-x}N_x$ layers [3,4] by TEM and HRXRD, while for lower N contents the layers were found to be homogeneous.

The DF obtained for our buffer GaP layer, and consequently the absorption coefficient spectrum deduced for the GaP sample test in Fig. 3, are quite similar to previously reported data for GaP by Jellison in the range $1.476 \leq E \leq 5.6$ eV [13]. Both DF curves (from Jellison and this work) are available in the supporting information section. The GaP

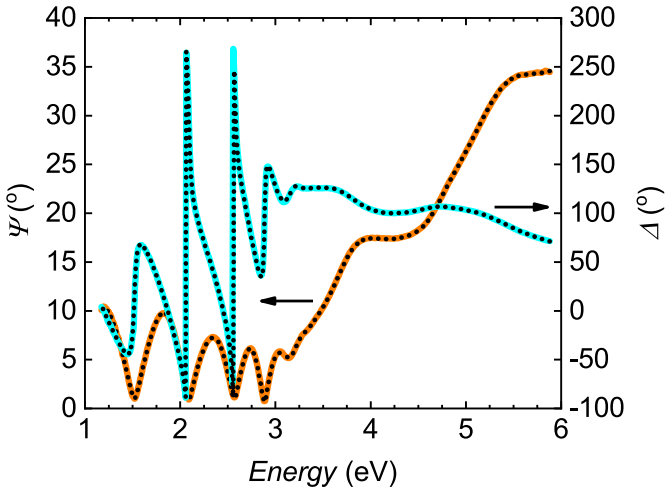

Fig. 2. Example of SE measurement fit to a three-layer model (sample with $x = 0.024$). Continuous lines represent ellipsometric Ψ and Δ measurements, while dotted lines are the best generated fit.

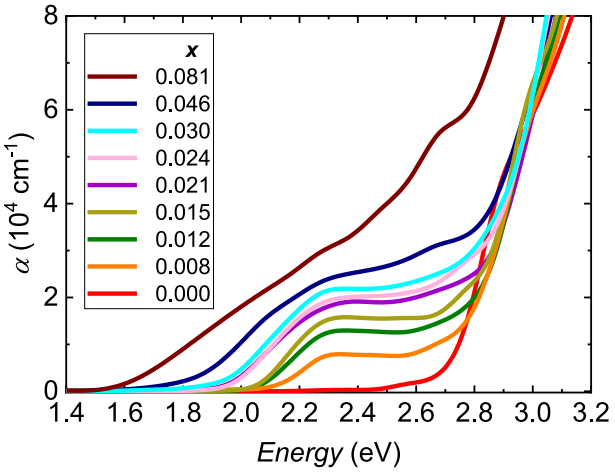

Fig. 3. Absorption coefficient spectra obtained for some $GaP_{1-x}N_x$ layers. Curves for $x \leq 0.03$ correspond to single-phase and homogeneous layers.

indirect and fundamental bandgap (X) absorption slowly increases from $E_X = 2.26$ eV, as expected for an indirect bandgdap. A more intense absorption edge around 2.78 eV, related to the direct GaP bandgap (Γ), is also clearly seen. These results validate our procedure and allow us to use this curve as library spectrum for our GaP buffer layer. The effects of the compressive strain of the GaP layer grown on Si substrate are expected to slightly shift the absorption edges.

Though these shifts are not expected to be very significant, they are included in the experimentally obtained library spectra.

The absorption coefficient spectrum for the sample with $x = 0.021$ (lattice-matched to the Si substrate) is clearly similar to that previously obtained by Shokhovets et al. [14] for the same x value, although the sample growth method and the procedure followed for SE data analysis are different. This agreement further validates our procedure, including both, the proposed model and GaP library data.

Three main features can be appreciated when comparing the set of curves shown in Fig. 3. First, a red shift of the absorption edge is observed with increasing N mole fraction, indicating a reduction of the bandgap energy from the initial GaP value. Second, a plateau region is formed between 2.3 and 2.6 eV, just above the absorption edge; this plateau is only well-defined for samples with $x \leq 0.03$, i.e., for single-phase samples. Third and finally, a monotonic increase of the value of the absorption coefficient is observed in the plateau region as the N content is increased. For samples with the higher x values, the plateau region is progressively replaced by a generalized absorption increase.

The above three observed characteristics are compatible with the formation of a direct bandgap in $GaP_{1-x}N_x$ which lies below the indirect GaP bandgap energy E_X, as previously observed and proposed by the BAC model applied to this ternary alloy [2]. This model, when applied to dilute nitrides, is based on the weak coupling between N localized states and extended states of the conduction band in the host semiconductor matrix, GaP in our case, that modifies the original Hamiltonian [15]. Using first order perturbation theory, the new Hamiltonian can be represented in matrix form -using the basis of unperturbed states of the conduction band and the isolated nitrogen level in the host semiconductor- as

$$\begin{pmatrix} E_M(\boldsymbol{k}) & V_{NM} \\ V_{NM} & E_N \end{pmatrix} \quad (3)$$

where $E_M(\boldsymbol{k})$ is the energy of the host GaP conduction band, E_N is the energy of the N impurity level, and V_{NM} is the matrix element representing the interaction between both states.

This non-diagonal term may be stated as

$$V_{NM} = C_{NM}\, x^{1/2} \tag{4}$$

where x is N mole fraction.

It has been proposed by some authors [16,17] a dependence of the coupling parameter C_{NM} on the electron wave vector $\boldsymbol{k}$ in the form:

$$C_{NM}(\boldsymbol{k}) = \frac{C_{NM}(0)}{\left(1 + l_d^2 k^2\right)^2} \tag{5}$$

where l_d is a constant of the order of the lattice constant. Under this model, $C_{NM}(\boldsymbol{k})$ decreases with $|\boldsymbol{k}|$, taking values 3–4 times smaller at X or L points than that at the Γ point [16,17].

Hamiltonian matrix diagonalization by solving the associated eigenvalues problem leads to two new energies for the conduction bands

$$E_{\pm}(\boldsymbol{k}) = \frac{1}{2}\left[E_N + E_M(\boldsymbol{k}) \pm \sqrt{\left(E_N - E_M(\boldsymbol{k})\right)^2 + 4C_{NM}^2(\boldsymbol{k})x}\right] \tag{6}$$

The energy E_N of the N isolated impurity in $GaP_{1-x}N_x$ lies in the bandgap, at 2.32 eV above the valence band maximum for low temperatures. The density of N-N nearest neighbor pairs with different distances (NN_i) raises as x is increased, reducing progressively that energy up to $E_N = 2.185$ eV [18,19] for the shorter distance pair NN_1 [20], value that can be used in the BAC model as the origin of the N band. Focusing on the lower energy branch $E_-(\boldsymbol{k})$, its energy starts to decrease from the $E = E_N$ value in the $x \to 0$ limit, for any $\boldsymbol{k}$ value. Nevertheless, considering the C_{NM} decrease with $|\boldsymbol{k}|$, the lowest energy for the new band will take place at Γ point ($\boldsymbol{k} = 0$), resulting in a direct bandgap whose energy decreases as the N content in the layer is increased.

The behavior predicted by Eq. (6) is observed in the absorption edge of the curves shown in Fig. 3, where the absorption edge is progressively red-shifted towards energies below the GaP absorption edge at E_X.

For bulk semiconductors with a direct bandgap, the dependence of the band-to-band light absorption coefficient on photon energy (for $\hbar\omega \geq E_g$) can be obtained from the Fermi's golden rule and the joint density of states of the conduction and valence bands as [21]

$$\alpha(E) = \frac{q^2 {m_0}^{1/2}}{4\pi\hbar^2 \varepsilon_0 c n_r}\left(\frac{2m_r}{m_0}\right)^{3/2} \frac{2{P_{CV}}^2}{m_0} \frac{\left(E - E_g\right)^{1/2}}{E} \tag{7}$$

where q is the electron charge, m_0 is the electron mass, $\hbar$ is the reduced Planck's constant, ε_0 is the vacuum permittivity, c is the speed of the light in the vacuum, n_r is the material refractive index, m_r is the reduced electron-hole effective mass, E is the photon energy, E_g is the direct bandgap energy, and P_{CV} is the momentum matrix element between the initial valence band state and the final conduction band state

$$P_{CV} = \langle \varphi_{CB}(k) | \mathbf{P} | \varphi_{VB}(k) \rangle \tag{8}$$

For most semiconductors, P_{cv} is not strongly dependent on the composition, but this is not the case for dilute nitrides, where this parameter is greatly dependent on N content [22], as we will discuss later.

The excitonic absorption contribution should be included in the absorption coefficient, particularly for low temperatures, where sharp peaks related to bound excitons should be observed below the bandgap energy. In our case, since measurements have been done at room temperature, that contribution is not evident in the spectra shape, due to thermal dissociation of bound excitons [23]. Nevertheless, excitonic absorption by continuum states -Sommerfeld enhancement [24–26]- increases the optical absorption above the bandgap. As the resulting energy dependence of the final absorption coefficient [25] is not appreciably changed, we have neglected the Sommerfeld enhancement for simplicity, because it should not significantly affect the obtained results.

According to Eq. (7), the bandgap energy E_g may be obtained as the horizontal intercept value of the linear extrapolation of $\alpha^2(E)E^2$ near the absorption edge. Fig. 4 is a plot of $\alpha^2(E)E^2$ versus E for some of the samples in the region near the absorption edge. For layers previously identified as single-phase samples ($x \leq 0.03$), a clear linear dependence is observed in the region near the absorption edge, confirming the direct nature of the bandgap in $GaP_{1-x}N_x$. An absorption tail below the bandgap energy -known as Urbach tail [27]- is also noticed in those curves, exhibiting the reported exponential decay of the absorption coefficient in that region.

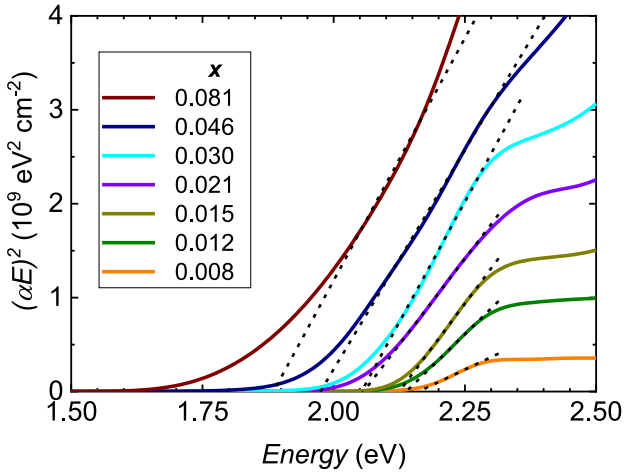

Fig. 4. Linear fitting of $(\alpha(E)E)^2$ from absorption data of $GaP_{1-x}N_x$ layers.

It is also clear from Fig. 4 that the direct bandgap energy decreases with N content, but it is even more evident in Fig. 5, where we have plotted the obtained E_g values versus the N content using squares as symbols (black squares). The obtained bandgap energy values for phase-separated layers (orange square) cannot be directly correlated with their averaged N concentrations; regions with different slopes could be identified in $\alpha^2(E)E^2$ curves for these layers, which are probably related to different bandgap energy values for each phase.

Fig. 5 also shows for comparison peak energy values obtained from PL spectra taken at $T = 14$ K (blue and orange triangles). PL transition energies are associated to bandgap recombining transitions between conduction and valence band, or near bandgap transitions often mediated by excitons, shallow impurity levels or band localized states. As can be seen in this figure, E_g values obtained by SE at room temperature are about 50–100 meV higher than transition energies obtained from PL

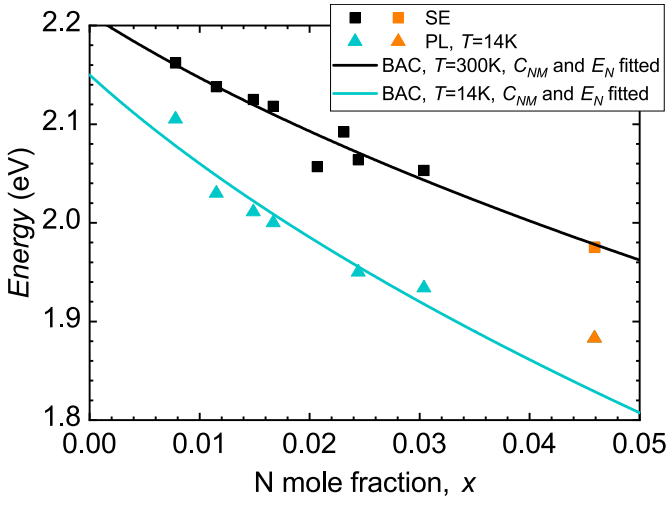

Fig. 5. Energy values obtained from SE measurements at room temperature according to Eq. (7) and PL measurements. The blue and black lines are the best PL and SE data fitting to the BAC model.

peaks at $T = 14$ K.

In terms of bandgap energy, this behavior is contrary to the observed trend for semiconductors, including $GaP_{1-x}N_x$, as the bandgap energy decreases when the temperature is increased. Indeed, for $GaP_{1-x}N_x$, the bandgap energy reduction between 12 K and 300 K can be calculated from Eq. (6) and available data [28,29], obtaining values ranging from 0 to 26 meV when N is incorporated up x = 0.03.

Observed discrepancies between the energies of both optical measurements are likely related to the origin of PL transitions in $GaP_{1-x}N_x$ alloys, arising from N-related localized states instead of band-to-band recombination or free exciton recombination [30]. More specifically, N local concentration fluctuations could result in a tail of localized states below the conduction band, trapping electrons before they recombine at lower energies than the bandgap. Carbon acceptor impurities, always detected in our samples grown by CBE using metalorganic precursors, could also be responsible for the main PL peak, associated to the (e,A^o) transition [31]. In both cases, either PL emission from N localized states or from C impurities, the PL peak energy is lowered.

The blue line in Fig. 5 represents the best fit of the BAC model given by Eq. (6) to PL peak energies with $E_M = E_\Gamma$ ($T = 12$ K) = 2.87 eV, while E_N and C_{NM} were fitting parameters, obtaining the values $E_N = 2.15 \pm 0.03$ eV and $C_{NM} = 2.7 \pm 0.2$ eV. A relatively good agreement is observed between these data and those previously obtained by Shan et al. [2] at room temperature ($E_N = 2.18$ eV, $C_{NM} = 3.05$ eV).

The upper black curve in Fig. 5 is a similar fitting to E_g from SE data with $E_M = E_\Gamma$ ($T = 300$ K) = 2.78 eV, obtaining the values $E_N = 2.22 \pm 0.02$ eV and $C_{NM} = 2.1 \pm 0.2$ eV; this last one is lower than the more usually reported values between 3.05 [2,17,29] and 4.38 eV [32], and even to that of Buyanova et al. [33] of 2.76 eV.

In our previous work [34], taking into account carrier localization, the best fit of the BAC model to PL measurements with a similar sample set of single-phase samples yields to $C_{NM} = 2.24$ eV, in good agreement with the value obtained from SE fit. Since C_{NM} has been usually obtained by several experimental techniques, as photoreflectance or photomodulated transmission spectroscopies, and as in the case of the bandgap value, it could be dependent on the specific optical technique. Phase separation in $GaP_{1-x}N_x$ layers and the added difficulty for the precise N substitutional mole fraction measurement by using techniques such as HRXRD, TEM and nuclear reaction analysis may be other factors for the observed discrepancy.

It is worth noting that E- value should progressively approach to the E_N value when N content is reduced, independently of sample temperature, as predicted by Eq. (6). The black curve in Fig. 5 also suggests a value for E_N (2.22 eV) slightly larger than the usual value (2.18 eV). This difference could be related to the temperature dependence of E_N, as it has been also proposed for the GaInAsN system [35,36].

The effect of the strain on bandgap energy can be calculated from available data [28,29], inducing a bandgap reduction which is almost negligeable for $x < 0.021$. For larger x values, the bandgap energy is progressively reduced up to about 12 meV for $x = 0.03$. Since strain would affect to both, SE and PL data, the observed PL-SE energy shift cannot be attributed to the strain present in the layers. Nevertheless, the reduction of the band gap caused by strain could affect the obtained C_{NM} value.

From data in Fig. 3, $GaP_{1-x}N_x$ layers show a strong absorption coefficient due to their direct bandgap. Absorption coefficient values of around 5×10^3 cm^{-1} near E_g are comparable to those of high efficiency solar cell materials [37]. It is worth to notice that α values shown in Fig. 3, even for the lower N contents of single-phase samples, suggest that $GaP_{1-x}N_x$ layers are suitable to be used as topmost absorber on Si-based tandem solar cells. Indeed, for a $GaP_{1-x}N_x$ layer as topmost solar cell with $x \geq 0.02$ ($\alpha \geq 2 \times 10^4$ cm^{-1}), a thickness $d = 3\alpha^{-1} \leq 1.5$ μm could be used for 95 % light absorption above the $GaP_{1-x}N_x$ bandgap, allowing the use of thin epitaxial layers. Moreover, a bandgap of 1.95 eV could be obtained for N contents about 0.04–0.05 (Fig. 5) which is ideal for a constrained tandem $GaP_{1-x}N_x$ solar cell epitaxially grown over the lower Si cell.

There are some published works reporting measurements on the absorption coefficient on GaP-based dilute nitrides layers such as $GaP_{1-x}N_x$ or $GaP_{1-x-y}As_yN_x$, obtaining α values around 1-2x10^4 cm^{-1} in the plateau region above the bandgap energy, but they do not show a clear trend of the absorption coefficient evolution when changing the N mole fraction [8–10].

Near the absorption threshold, $E = E_g$, considering the variation of n_r with the photon energy for each sample is only of the order of 2 % in this region, $\alpha^2(E)$ Taylor's approximation of Eq. (7) is

$$\alpha^2(E) \approx \alpha_0^2 \frac{E - E_g}{E_g} \tag{9}$$

with

$$\alpha_0 = \frac{q^2 {m_0}^{1/2}}{4\pi\hbar^2 \varepsilon_0 c n_r} \left(\frac{2m_r}{m_0}\right)^{3/2} \frac{2{P_{CV}}^2}{m_0} \frac{1}{\sqrt{E_g}} \tag{10}$$

The parameter α_0 is an indicator of the light absorption strength in the layer. Its value may be obtained as the slope of the linear fitting of $\alpha^2(E)$ near the absorption edge, from a plot like Fig. 4. The obtained values for α_0 coefficient from the slope of $\alpha^2(E)$ for some of the $GaP_{1-x}N_x$ layers as a function of the N content are plotted in Fig. 6. A monotonically increasing behavior with the N mole fraction is observed for samples with single-phase. This behavior may be associated to the structure of the new $GaP_{1-x}N_x$ bands near the Brillouin zone center.

The new eigenstates of the perturbed Hamiltonian represented in Eq. (3) are a hybridization of the original unperturbed states; particularly, for the lower energy conduction band (E_-), the new state could be written as

$$|\varphi_-(\boldsymbol{k})\rangle = a_- |\varphi_M(\boldsymbol{k})\rangle + b_- |\varphi_N\rangle \tag{11}$$

where $|\varphi_M(\boldsymbol{k})\rangle$ and $|\varphi_N\rangle$ are the basis of the conduction band and the isolated nitrogen level unperturbed states in the host semiconductor, respectively. A similar result is obtained for the upper energy state $|\varphi_+(\boldsymbol{k})\rangle$ after a permutation of both coefficients, a_- and b_-, whose squared moduli are obtained as

$$|a_-|^2 = \frac{1}{2}\left(1 - \frac{1}{\sqrt{1 + \frac{4\,{C_{NM}}^2 x}{(E_M(\boldsymbol{k}) - E_N)^2}}}\right), |b_-|^2 = 1 - |a_-|^2 \tag{12}$$

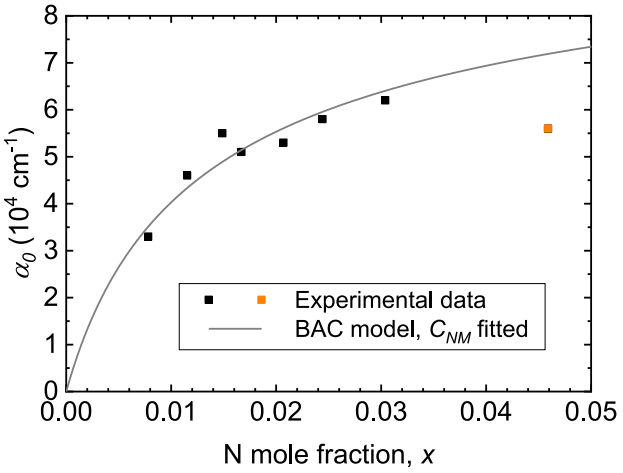

Fig. 6. α_0 values obtained from SE measurements at room temperature for $x \leq 0.05$ and best C_{NM} fitting for single-phase samples (black points, $x \leq 0.03$) to Eq. (15), with $E_\Gamma = E_M = 2.78$ eV and $E_N = 2.22$ eV.

It is important to point out that the GaP component of the new lower conduction band state $|\varphi_-(\boldsymbol{k})\rangle$ is given by $|a_-|^2$, which is an increasing function of x, taking values between $|a_-|^2 = 0$ (for $x = 0$) and $|a_-|^2 = 0.5$ for $x \gg ((E_M(\boldsymbol{k}) - E_N)/2C_{NM})^2$. For the single-phase layer with the larger N-content studied in this work ($x = 0.03$), this GaP component may be estimated as $|a_-|^2 \approx 0.25$, which is half of the maximum allowed value.

Returning to Eq. (7), n_r and m_r are expected to show a slow variation with the N content of the layers, being approximately constants in the range of x values shown in Fig. 6. A similar approximation could also be done for $E_g^{1/2}$ values of our sample set. Under these assumptions, the square of momentum matrix element, P_{CV}^2, should be the main responsible for the observed α_0 dependence on x. Since reported values of this parameter for different binary semiconductors, given in energy units as

$$E_P = \frac{2\, m_0}{\hbar^2} P_{CV}{}^2 \tag{13}$$

are in the range between 15 and 30 eV [28], the optical absorption strength does not change significantly with composition in most ternary and quaternary semiconductors. This is not the case for the $GaP_{1-x}N_x$ layers studied in this work, where a small change in x from 0.008 to 0.03 almost doubles the value of α_0.

The optical response functions for $GaP_{1-x}N_x$ and $GaP_{1-y}As_y$ have been obtained by Zou and Goodnick [22] after tight binding calculations of their electronic band structure. Data reported in that work for $P_{CV}^2(x)$ show a behavior quite similar to $|a_-|^2$, as given by Eq. (12).

For the lower conduction band states in $GaP_{1-x}N_x$, combining Eqs. (8) and (11), P_{CV} is obtained as

$$P_{CV} = a_-\, P_{CV}(\mathrm{GaP}) + b_-\, P_{NV} \tag{14}$$

where P_{CV}(GaP) and P_{NV} are the momentum matrix elements of the host GaP direct bandgap and the N to valence band transition, respectively. Considering the dependence of both $|a_-|$ and $|b_-|$ on x, the contribution of the GaP-like Γ transition would be progressively increased as more N is incorporated into the layer, while simultaneously the N-like contribution would decrease.

The N content dependence of the absorption strength data plotted in Fig. 6 also has a similar behavior to $|a_-|^2$, as is given by Eq. (12), revealing the stronger Γ component of $|\varphi_-(\boldsymbol{k})\rangle$ when increasing the N content, as suggested by W. Shan et al. [15]. Features due to the $|\varphi_N\rangle$ contribution to the layer absorption, expected to be smaller, would also be attenuated by the corresponding decreasing term $|b_-|^2$.

Neglecting the contribution of P_{NV} to P_{CV} in Eq. (14), the optical absorption coefficient strength for $GaP_{1-x}N_x$ layers could then be approximated to:

$$\alpha_0 = \alpha_{0(GaP)} \cdot |a_-|^2 \tag{15}$$

The solid line in Fig. 6 represents the best fit for the experimental α_0 data to the above equation for single-phase layers (black squares symbols). We have used for that fitting $E_{\Gamma} = E_M(T = 300\ \mathrm{K}) = 2.78$ eV, the obtained value $E_N = 2.22$ eV from Fig. 5 data fitting, and the value $\alpha_0(GaP) = 2.27 \times 10^5\ \mathrm{cm}^{-1}$ taken from our own library spectrum -similar to a previously reported value [13]- with the only fitting parameter C_{NM}. The obtained value, $C_{NM} = 3.3 \pm 0.1$ eV, is also close to previously reported values.

The resulting 50 % difference between both calculated values for the C_{NM} coupling parameter (from absorption band edge and from absorption strength) is not clearly understood. According to the BAC model, as C_{NM}, E_M and E_N are material-related constants, microscopic fluctuations of the N content could be responsible of small local changes on the E_N value [18,19] and also on the obtained C_{NM} value.

4. Conclusions

We have obtained by spectroscopic ellipsometry the optical properties of epitaxial $GaP_{1-x}N_x$ layers grown on GaP/Si(001) substrates with N mole fractions in the range $0 \le x \le 0.081$. Absorption coefficient spectra of these layers show direct-like bandgap behavior for $x > 0$, while the absorption edge decreases as the N content is increased, both in agreement with the band anticrossing model. In single-phase layers with homogeneous N content, the absorption coefficient shows a plateau just above the absorption edge. Values of the absorption coefficient, around $1\text{-}2\text{x}10^4\ \mathrm{cm}^{-1}$ in the plateau region, increase with N content, being suitable for using $GaP_{1-x}N_x$ epitaxial layers as topmost absorber on Si-based tandem solar cells. Both E_g and α_0 parameters have been deduced from the absorption spectra for the set of samples. Obtained E_g values for all the samples are up to 100 mV greater than those obtained at 14 K by photoluminescence, probably due carrier localization associated to local N concentration fluctuations or to impurity mediated recombination. The observed $E_g(x)$ dependence allows to obtain the BAC parameter $C_{NM} = 2.1$ eV, lower than values previously reported. The dependence of the optical absorption strength, $\alpha_0(x)$, reproduces the increasing Γ character of the electronic wave function in the conduction band as x is increased, allowing to obtain a C_{NM} value of 3.3 eV, much closer to those already reported.

CRediT authorship contribution statement

K. Ben Saddik: Writing – review & editing, Writing – original draft, Investigation. **M.J. Hernández:** Writing – review & editing, Writing – original draft, Investigation. **M.A. Pampillón:** Writing – review & editing, Writing – original draft, Investigation. **M. Cervera:** Writing – review & editing, Writing – original draft, Investigation. **B.J. García:** Writing – review & editing, Writing – original draft, Investigation, Funding acquisition.

Declaration of competing interest

The authors declare the following financial interests/personal relationships which may be considered as potential competing interests:

B. J. Garcia reports financial support was provided by Spanish Ministry of Science and Innovation. If there are other authors, they declare that they have no known competing financial interests or personal relationships that could have appeared to influence the work reported in this paper.

Acknowledgments

Authors acknowledge S. Fernández-Garrido for his contribution to the growth of some samples and T. Vallés for technical assistance. This research has been supported by the Spanish Ministry of Science and Innovation under Project No. PID2020-114280RB-I00.

Appendix A. Supplementary data

Supplementary data to this article can be found online at https://doi.org/10.1016/j.mssp.2024.109011.

Data availability

Data will be made available on request.

References

[1] W. Walukiewicz, J.M.O. Zide, Highly mismatched semiconductor alloys: from atoms to devices, J. Appl. Phys. 127 (2020) 010401, https://doi.org/10.1063/1.5142248.

[2] W. Shan, W. Walukiewicz, K.M. Yu, J. Wu, J.W. Ager, E.E. Haller, H.P. Xin, C. W. Tu, Nature of the fundamental band gap in GaN_xP_{1-x} alloys, Appl. Phys. Lett. 76 (2000) 3251, https://doi.org/10.1063/1.126597.

[3] K. Ben Saddik, S. Fernández-Garrido, R. Volkov, J. Grandal, N. Borgardt, B. J. García, Growth modes and chemical-phase separation in $GaP_{1-x}N_x$ layers grown by chemical beam epitaxy on GaP/Si(001), J. Appl. Phys. 134 (2023) 175703. https://doi:10.1063/5.0173748.

[4] K. Ben Saddik, B.J. García, S. Fernández-Garrido, A growth diagram for chemical beam epitaxy of $GaP_{1-x}N_x$ alloys on nominally (001)-oriented GaP-on-Si substrates, Apl. Mat. 9 (12) (2021) 121101, https://doi.org/10.1063/5.0067209.
[5] K. Ben Saddik, A.F. Braña, N. López, W. Walukiewicz, B.J. García, Growth of $GaP_{1-x-y}As_yN_x$ on Si substrates by chemical beam epitaxy, J. Appl. Phys. 126 (10) (2019) 105704, https://doi.org/10.1063/1.5111090.
[6] K. Kharel, A. Freundlich, Band structure and absorption properties of (Ga, In)/(P, As, N) symmetric and asymmetric quantum wells and super-lattice structures: towards lattice-matched III-V/Si tandem, J. Appl. Phys. 124 (2018) 095104, https://doi.org/10.1063/1.5040858.
[7] M. Yamaguchi, F. Dimroth, John F. Geisz, N.J. Ekins-Daukes, Multi-junction solar cells paving the way for super high-efficiency, J. Appl. Phys. 129 (2021) 240901, https://doi.org/10.1063/5.0048653.
[8] R. Kudrawiec, A.V. Luce, M. Gladysiewicz, M. Ting, Y.J. Kuang, C.W. Tu, O. D. Dubon, K.M. Yu, W. Walukiewicz, Electronic band structure of $GaN_xP_yAs_{1-x-y}$ highly mismatched alloys: suitability for intermediate-band solar cells, Phys. Rev. Appl. 1 (2014) 034007, https://doi.org/10.1103/PhysRevApplied.1.034007.
[9] H.P. Xin, C.W. Tu, Y. Zhang, A. Mascarenhas, Effects of nitrogen on the band structure of GaN_xP_{1-x} alloys, Appl. Phys. Lett. 76 (2000) 1267, https://doi.org/10.1063/1.126005.
[10] K. Zelazna, M. Gladysiewicz, M.P. Polak, S. Almosni, A. Létoublon, C. Cornet, O. Durand, W. Walukiewicz, R. Kudrawiec, Nitrogen-related intermediate band in P-rich $GaN_xP_yAs_{1-x-y}$ alloys, Sci. Rep. 7 (2017) 15703, https://doi.org/10.1038/s41598-017-15933-1.
[11] C.M. Herzinger, B. Johs, W.A. McGahan, J.A. Woollam, W. Paulson, Ellipsometric determination of optical constants for silicon and thermally grown silicon dioxide via a multi-sample, multi-wavelength, multi-angle investigation, J. Appl. Phys. 83 (1998) 3323, https://doi.org/10.1063/1.367101.
[12] S. Zollner, Model dielectric functions for native oxides on compound semiconductors, Appl. Phys. Lett. 63 (18) (1993) 2523, https://doi.org/10.1063/1.110469.
[13] G.E. Jellison Jr., Optical functions of GaAs, GaP, and Ge determined by two-channel polarization modulation ellipsometry, Opt. Mater. 1 (1992) 151.
[14] S. Shokhovets, O. Supplie, C. Koppka, S. Krischok, T. Hannappel, Optical constants and origin of the absorption edge of GaPN lattice-matched to Si, Phys. Rev. B 98 (2018) 075205, https://doi.org/10.1103/PhysRevB.98.075205.
[15] W. Shan, W. Walukiewicz, J.W. Ager, E.E. Haller, J.F. Geisz, D.J. Friedman, J. M. Olson, S.R. Kurtz, Band anticrossing in GaInNAs alloys, Phys. Rev. Lett. 82 (1999) 1221, https://doi.org/10.1103/PhysRevLett.82.1221.
[16] J. Wu, W. Walukiewicz, E.E. Haller, Band structure of highly mismatched semiconductor alloys: coherent potential approximation, Phys. Rev. B 65 (2002) 233210, https://doi.org/10.1103/PhysRevB.65.233210.
[17] J. Wu, W. Walukiewicz, K.M. Yu, J.W. Ager, E.E. Haller, Y.G. Hong, H.P. Xin, C. W. Tu, Band anticrossing in $GaP_{1-x}N_x$ alloys, Phys. Rev. B 65 (2002) 241303, https://doi.org/10.1103/PhysRevB.65.241303.
[18] D.G. Thomas, J.J. Hopfield, Isoelectronic traps due to nitrogen in gallium phosphide, Phys. Rev. Lett. 15 (1965) 857, https://doi.org/10.1103/PhysRevLett.15.857.
[19] D.G. Thomas, J.J. Hopfield, Isoelectronic traps due to nitrogen in gallium phosphide, Phys. Rev. 150 (1966) 680, https://doi.org/10.1103/PhysRev.150.680.
[20] J.N. Baillargeon, P.J. Pearah, K.Y. Cheng, G.E. Hofler, K.C. Hsieh, Growth and luminescence properties of GaP:N and $GaP_{1-x}N_x$, J. Vac. Sci. Techn. B 10 (1992) 829, https://doi.org/10.1116/1.586127.
[21] P. Bhattacharya, Semiconductor Optoelectronic Devices, second ed., Prentice Hall, New Jersey, 1997, p. 124.
[22] Y. Zou, S.M. Goodnick, Calculation of optical response functions of dilute-N GaPAsN lattice-matched to Si, J. Appl. Phys. 127 (2020) 075703, https://doi.org/10.1063/1.5140482.
[23] M.D. Sturge, Optical absorption of gallium arsenide between 0.6 and 2.75 eV, Phys. Rev. 127 (1962) 768, https://doi.org/10.1103/PhysRev.127.768.
[24] R.J. Elliott, Intensisty of optical absorption by excitons, Phys. Rev. 108 (1957) 1384, https://doi.org/10.1103/PhysRev.108.1384.
[25] P.Y. Yu, M. Cardona, Fundamentals of Semiconductors: Physics and Materials Properties, fourth ed., Springer Berlin Heidelberg, 2010 https://doi.org/10.1007/978-3-642-00710-1. Chap.6.
[26] C. Emminger, N.S. Samarasingha, M. Rivero Arias, F. Abadizaman, J. Menéndez, S. Zollner, Excitonic effects at the temperature-dependent direct bandgap of Ge, J. Appl. Phys. 131 (2022) 165701, https://doi.org/10.1063/5.0080158.
[27] S.R. Johnson, T. Tiedje, Temperature dependence of the Urbach edge in GaAs, J. Appl. Phys. 78 (1995) 56098, https://doi.org/10.1063/1.359683.
[28] I. Vurgaftman, J.R. Meyer, L.R. Ram-Mohan, Band parameters for III–V compound semiconductors and their alloys, J. Appl. Phys. 89 (2001) 5815, https://doi.org/10.1063/1.1368156.
[29] I. Vurgaftman, J.R. Meyer, Band parameters for nitrogen-containing semiconductors, J. Appl. Phys. 94 (2003) 3675, https://doi.org/10.1063/1.1600519.
[30] J. Plaza, J.L. Castaño, B.J. García, H. Carrère, E. Bedel-Pereira, Temperature dependence of photoluminescence and photoreflectance spectra of dilute GaAsN alloys, Appl. Phys. Lett. 86 (2005) 121918, https://doi.org/10.1063/1.1891293.
[31] K. Ben Saddik, A.F. Braña, N. López, B.J. García, S. Fernández-Garrido, Growth of silicon- and carbon-doped GaAs by chemical beam epitaxy using H2-diluted DTBSi and CBr_4 precursors, J. Cryst. Growth 571 (2021) 126242, https://doi.org/10.1016/j.jcrysgro.2021.126242.
[32] J. Chamings, S. Ahmed, A.R. Adams, S.J. Sweeney, V.A. Odnoblyudov, C.W. Tu, B. Kunert, W. Stolz, Band anti-crossing and carrier recombination in dilute nitride phosphide based lasers and light emitting diodes, Phys. Stat. Sol. B 246 (2009) 527, https://doi.org/10.1002/pssb.200880537.
[33] I.A. Buyanova, M. Izadifard, A. Kasic, Analysis of band anticrossing in GaN_xP_{1-x} alloys, Phys. Rev. B 70 (2004) 085209, https://doi.org/10.1103/PhysRevB.70.085209.
[34] K. Ben Saddik, P. Alamo, J. Lahnemann, R. Volkov, N.I. Borgardt, T. Flissikowski, O. Brandt, B.J. Garcia, S. Fernandez-Garrido, in: 2022 Compound Semiconductor Week (CSW), IEEE, Ann Arbor, MI, USA, 2022, pp. 1–2, https://doi.org/10.1109/CSW55288.2022.9930454.
[35] C. Skierbiszewski, P. Perlin, P. Wisniewski, T. Suski, J.F. Geisz, K. Hingerl, W. Jantsch, D.E. Mars, W. Walukiewicz, Band structure and optical properties of InyGa1-yAs1-xNx alloys, Phys. Rev. B 65 (2001) 035207, https://doi.org/10.1103/PhysRevB.65.035207.
[36]] A. Grau, T. Passow, M. Hetterich, Temperature dependence of the GaAsN conduction band structure, Appl. Phys. Lett. 89 (2006) 202105, https://doi.org/10.1063/1.2387973.
[37] H. Fujiwara, R.W. Collins (Eds.), Spectroscopic Ellipsometry for Photovoltaics: Volume 2: Applications and Optical Data of Solar Cell Materials, Springer International Publishing, Cham, 2018.